

Environmental Sustainability of Arctic Shipping through Potential HFO-banned Areas along the NSR

Chathumi Ayanthi Kavirathna¹, Ryuichi Shibasaki¹, Wenyi Ding², Natsuhiko Otsuka³

¹ Resilience Engineering Research Center (The University of Tokyo, Tokyo, Japan)

² Department of Systems Innovation (The University of Tokyo, Tokyo, Japan)

³ Arctic Research Center (Hokkaido University, Hokkaido, Japan)

ABSTRACT

Owing to the emergent trends in Arctic shipping, different market and policy-based measures would be considered to minimize the negative impacts from vessel-based emissions to the fragile Arctic sea environment. This study analyzes the effectiveness of enforcing HFO-banned areas and emission tax for the environmental sustainability of Arctic shipping. The locations of potential HFO-banned areas are analyzed with an optimization model to minimize the total emissions and cost separately and three scenarios are analyzed with free-ice, medium-ice, and heavy-ice conditions based on daily ice-thickness data obtained from the Arctic Data Archive-TOPAZ4 system. The analysis is done for a voyage from Asia to Europe and vessel speeds and location data are gathered from the Automatic Identification System (AIS). Vessel-based emissions are estimated following the IMO fourth GHGs study in 2020 which incorporates the vessel's engine load, propulsive power demanded at different speeds, and fuel consumption with auxiliary engines and boilers, among others. A spatial variation of the selected HFO-banned areas is observed when changing ice conditions while producing different levels of CO₂, CH₄, N₂O, BC, and SO_x emissions. Although the enforcement of HFO-banned areas and emission tax reduces the total emissions, it significantly increases the total cost of the voyage. The medium-ice condition generates the least emission level and significantly different results are derived from environmental and economic objectives with all scenarios.

KEYWORDS: Environmental sustainability, Arctic shipping, HFO-banned areas, Vessel-based emissions

INTRODUCTION

The Arctic shipping receives considerable attention from practitioners and scholars owing to the dramatic retreat of sea ice driven by global warming (Theocharis et al., 2019). Therefore, the Northern Sea Route (NSR) is being developed as an attractive route in the global shipping market considering its distance- and time-saving effects than conventional shipping routes especially when facilitating cargo movements between Asia and Europe (Xu et al., 2018). Despite the economic advantages, significant environmental issues would be expected when increasing traffic via NSR due to the adverse impacts from vessel-based emissions to the fragile Arctic sea environment. Therefore, various market- and policy-based measures are discussed by the regional and international bodies including International Maritime Organization (IMO) to minimize environmental issues from Arctic shipping.

Restricting the burning of Heavy Fuel Oil (HFO) is considered an important initiative due to the high emission factors for Green House Gases (GHG) with HFO. Thus, enforcing HFO-

banned areas and emission tax can be potential measures to minimize vessel-based emission with Arctic shipping. Although emissions can also be reduced by installations of scrubbers to filter exhaust gases, fuel switching is discussed as a cost-effective measure (Theocharis et al., 2019). Hence, this study assumes the switching from HFO to MGO (Marine Gas Oil) by vessels when navigating through HFO-banned areas along the NSR because MGO is considered more environmentally friendly than HFO (IMO, 2020). Therefore, the purpose of this study is to analyze the effectiveness of HFO-banned areas and emission tax for enhancing the environmental sustainability of Arctic shipping. To achieve this objective, we will estimate the total cost and emission levels for a given voyage considering scenarios with and without enforcing HFO-banned areas and emission tax. We consider both economic and environmental objectives separately when deciding HFO-banned areas and the sensitivity of different policy-related variables are analyzed. Further, three different scenarios are assumed with different ice-conditions given as free-ice, medium-ice, and heavy-ice, and the spatial variations of HFO-banned areas when changing the ice condition are analyzed considering both economic and environmental objectives. The remainder of this paper is organized as follows: Section 2 focuses on the literature view and Section 3 describes the methodology. Results and discussion are given in Section 4 and Section 5 concludes the paper.

LITERATURE REVIEW

Since this study analyzes the effectiveness of HFO-banned areas and emission tax with both environmental and economic objectives, previous related studies are summarized. Lindstad et al. (2016) compared the costs, emissions, and climate impacts for navigating via NSR and Suez Canal Route (SCR) and calculated the engine power and emission as a function of vessel speed and ice condition. Accordingly, vessel emissions offset the effect of shorter voyages, thus NSR would not generate climate benefits even with cleaner fuels. Yumashev et al. (2017) assessed the climate and economic feedback of NSR by determining NSR's navigability based on sea-ice prediction while feeding the navigability results into a business model. They estimated direct emissions reduction by NSR and indirect emissions generated from NSR-driven marginal economic growth. With big data mining, Zhang et al. (2018) assessed the exploitation of trans-Arctic routes while estimating sea ice concentration, ice extent, and ice thickness with satellite remote sensing. They decided vessel's speeds based on ice numeral to estimate navigation time and cost. Faury and Cariou (2016) considered monthly variations of ice conditions to analyze potential cost and time saving via NSR than SCR assuming speed as a function of ice-thickness and highlighted the NSR's advantages for summer navigation. Otsuka et al. (2013) analyzed whether the shipping cost saving via NSR could offset the cost caused by ice conditions. As per the results, the shortened distance of NSR could save the shipping cost because the costs of icebreakers and ice pilots do not largely exceed the Suez Canal fee. Xu et al. (2018) proposed a seasonal NSR-SCR combined service for using NSR only during its economical navigable window. They predicted the vessel's time for entering and exiting the ice-covered stage and calculated additional power requirements to overcome ice resistance considering the speeds at the ice-free stage and ice-water. Somanathan et al. (2009) compared the economics of shipping via the Northwest Passage and Panama canal route. They modeled ice conditions from historical records to estimate ship speeds at different navigation legs and estimated the required freight rate to recover all costs. Zhang et al. (2016) compared shipping efficiency between trans-arctic and conventional routes and analyzed the sensitivity of high fuel consumption due to heavy vessel and sea ice resistance. Accordingly, although NSR would save 10 days for a transit, container shipping loses its profit margin with NSR despite the cost-saving of oil shipping. Thus, previous studies highlighted both positive and negative aspects of Arctic shipping with diverse modeling approaches, which encourage us to further analyze the

effect of different policy-based measures to enhance the Arctic shipping feasibility in this study.

When considering previous studies that focused on different fuel types and emission tax, the speed optimization model of Theocharis et al. (2019) incorporated environmental policy in transition from high to low sulphur fuels and analyzed three scenarios; using HFO/MGO when operating outside/inside ECAs, using MGO, and installation of scrubber with HFO. Based on the findings, the MGO option mostly benefits NSR, and both the capital and operating cost increase when the vessel navigates at a speed slower than the optimal one regardless of fuel cost saving. Ding et al. (2020) analyzed the feasibility of NSR against SCR under fixed and progressive carbon tax schemes considering three fuel choices. Results highlighted that NSR is viable when the carbon tax is enforced or not enforced on both routes regardless of the tax schemes, although a progressive tax scheme is more preferred than the fixed one. Cariou et al. (2019) considered vessel's speed depended on the daily ice thickness from 2006 to 2016 along different NSR subzones and highlighted a higher CO₂ emission of NSR than SCR due to a gap between operating and design speed of the vessel. Despite the availability of previous studies on various aspects of NSR, none of them considered the locations of HFO-banned areas with environmental and economic objectives when changing the ice-condition along the NSR as focused from our study, which highlights the contribution of this study to the existing literature.

METHODOLOGY

The methodology consists of several steps as described in detail in the following sub-sections.

Deciding Navigation Legs for a Given Voyage and HFO-banned Areas

As the navigation legs/zones, the majority of previous studies considered 7 legs (Faury and Cariou, 2016; Zhang et al., 2016). However, this study considers numerous navigation legs (over 100) based on voyage distance as follows. As the initial step, we obtained the navigation path for a given voyage from AIS, and then, 20nm×20nm grids were created covering the entire navigation path. When deciding navigation legs for the route segment within NSR, if the navigation length inside a single grid is ≤ 15 nm, we combine it with before or after grid which has the lowest length to consider them as a single leg. However, when deciding navigation legs outside the NSR, we consider navigation length inside a single grid ≤ 50 nm as a condition for combining it with before or after grid. Thus, we maintain shorter lengths for legs inside NSR than outside to consider navigation speeds of NSR more precisely. Next, potential HFO-banned areas are decided only inside the NSR to cover all navigation paths. Although there are many possible arrangements of HFO-banned areas, this study considers 17 potential HFO-banned areas given from A-Q in Figure 1 with an example voyage. Several grids before the Bering straits are added as a potential HFO-banned area due to the high vessel traffic in this area.

Scenarios on Ice-conditions and Related Navigation Speeds

To decide scenarios on ice conditions, we obtained daily ice thickness data from 2018.07.01 to 2018.12.31 for each grid located along the navigation path from Arctic Data Archive-TOPA4. Then, we calculate the average ice-thickness for five days intervals. Three scenarios are assumed for ice-condition given as free-ice (Aug-Sep), medium-ice (Oct-early Nov), and heavy-ice (late Nov-Dec). Although ice-concentration has a significant influence on vessel navigation, this study considers only the ice-thickness level assuming 100% ice-concentration inside grids when navigating from October to December.

The navigation speeds for the free-ice scenario are directly obtained from AIS considering the vessel's actual navigation data (Aug-Sep) and the average of the speeds within each leg is

calculated because a vessel is assumed to have the same speed inside a single leg for the cost and emission estimation. However, the vessel's speeds at the medium and heavy ice conditions are assumed based on the ice-thickness, thus they depend on the vessel's position (leg l_n) at period t due to the ice thickness of leg l_n ($I_t^{l_n}$). Hence, after obtaining ice-thickness levels, the navigation speeds are estimated based on Equation (1) to (3) (Cariou et al., 2019). Here, four different ice thresholds; I_i^1 , I_i^2 , I_i^3 and I_i^4 are assumed, which are varied based on the vessel's ice-breaking capability. Thus, vessel i in leg l_n at period t can navigate without reducing speed if the ice-thickness of l_n ($I_t^{l_n}$) is lower than I_i^1 ($I_t^{l_n} < I_i^1$) and vessel's speed must be reduced to a level defined by Equation (1) if the ice-thickness level is in between I_i^1 and I_i^2 ($I_i^1 < I_t^{l_n} < I_i^2$). If the ice-thickness level satisfies $I_i^2 < I_t^{l_n} < I_i^3$ condition, vessel needs icebreaker assistance and the speed of the ice-breaker equals 12 knots and if it is under $I_i^3 < I_t^{l_n} < I_i^4$ condition, the speed of the ice-breaker reduces to 10 knots. However, if ice-thickness is greater than I_i^4 ($I_i^4 < I_t^{l_n}$), a vessel cannot pass through the leg l_n even with an ice-breaker. These thresholds on ice-thickness are obtained from the Japan Association of Marine Safety (2015). The variation of ice conditions and speeds directly influence the estimation of voyage cost and emissions, which are discussed in detail in the following sub-section.

$$S_{t,i}^{Op} = U \times \left(\frac{I_t^{l_n}}{100}\right)^V \quad (1)$$

$$U = S_i^d \times \left(\frac{100}{I_i^1}\right)^V \quad (2)$$

$$V = \frac{(\log(S_i^{Min}) - \log(S_i^d))}{(\log(I_i^4) - \log(I_i^1))} \quad (3)$$

Nomenclature

N, l_n, i	Number of legs, n^{th} leg of the voyage, and i^{th} vessel passing through NSR
t, T_i^L	Time of the year (out of 365 days, $t=1, 2, 3 \dots 365$) and voyage duration (hours)
$S_{t,l_n,i}^{Op}$	Average of the instantaneous operating speed of vessel i during leg l_n at time t
S_i^{Min}, S_i^d	The minimum speed and the design speed of vessel i
$F_{l_n,i}$	Total fuel consumption by vessel i during leg l_n
$SFC_{i,d}^{Main}, SFC_{i,l_n}^{Main}$	Specific fuel oil consumption of the main engine (g/k Wh) of vessel i base value and when navigating inside leg l_n
EL_{i,l_n}	Engine load of vessel i when navigating inside leg l_n
$P_{ref,i}^{Main}, P_{i,l_n}^{Main}$	Reference power and power demanded by the main engine (kW) of vessel i at leg l_n
P_i^{AuxEng}, P_i^{Boi}	Power of auxiliary engines and boilers, respectively of vessel i
$\gamma_{Auc}, \gamma_{Boi}$	Fractions of time for using auxiliary engines and boilers from the total navigation time
U, V	Vessel specific parameters
$I_t^{l_n}$	Ice thickness of the leg l_n at time t
$I_i^1, I_i^2, I_i^3, I_i^4$	Thresholds of ice thickness level for navigating of vessel i
$D_i^{l_n}$	Navigation distance of vessel i within the leg l_n for a given voyage
η_w, η_f	Weather and fouling correction factors
n, m	Relationship of vessel's power requirement with her speed and draught, respectively
$drf_{ref,i}, drf_{i,l_n}$	Reference draught and the instantaneous draught of the vessel i at leg l_n
δ_w	Correction factor on the speed-power relationship
$K_i, Oper_i, Fuel_i,$	Total capital cost, operating cost, fuel cost, emission tax, and ice-breaking cost,
Em_i, IB_i	respectively of vessel i for a given voyage
$Price_i^{NB}, LT_i$	Newbuilding price (USD) and lifetime (years) of vessel i

σ, ρ	Premiums on newbuilding price and operation cost respectively for ice-class vessels
B_n	No of NSR's zones that require ice-breaker assistance
b_i, GT_i	Ice-breaking cost per NSR's zone per unit GT and the gross tonnage of vessel i
f, FP_f	Types of fuel (HFO, MGO) and price of fuel type f (USD/Ton)
$e, EF_{f,e}$	Emission type ($e = CO_2, CH_4, N_2O, BC$) and emission factor of type e with fuel f
GWP_e, e_{Tax}	Global warming potential of emission type e and unit emission tax (USD/CO ₂ eTon)
$Emission_i, a$	Total emission from voyage (CO ₂ e Tons) and HFO-banned areas; $a = A, B, \dots Q$
δ_a^{HFO}	Binary variable to decide whether area a is an HFO-banned area or not
M, A_{max}	Number of HFO-banned areas that a vessel is passing through during a given voyage and maximum allowable number of HFO-banned areas
τ	Limit on SOx emission as a fraction of total fuel consumption

Estimating Cost and Emission Levels

Since the selection of HFO-banned areas is done considering both the environmental and economic objectives, this section describes the method of estimating cost and emission levels. The total cost function in Equation (4) consists of five components; capital cost, operating cost, fuel cost, emission tax, and ice-breaking cost for a voyage. Capital cost is calculated with Equation (5) similar to Xu et al. (2018), where σ is assumed as a premium for the new building price of the ice-class vessel. Equation (6) calculates the operating cost where ρ is assumed to consider the additional operating cost due to the ice-class vessels.

$$Cost_i = K_i + Oper_i + Fuel_i + Em_i + IB_i \quad (4)$$

$$K_i = \frac{\sigma \times T_i^L \times Price_i^{NB}}{LT_i \times 365 \times 24} \quad (5)$$

$$Oper_i = \rho \times 0.5 \times K_i \quad (6)$$

The third component of Equation (4) represents the fuel cost, which is significant due to our focus on emission level. Total fuel cost can be estimated with Equation (7) as the summation of fuel consumption at each leg multiplied by respective fuel prices. However, the type of fuel used in each leg is decided based on whether they are located inside an HFO-banned area or not, thus, δ_a^{HFO} equals to 1 if area a is an HFO-banned area and 0 otherwise. The total fuel consumption during a single leg can be estimated with Equation (8) considering the auxiliary engines and boilers as well. Here, γ_{Auc} and γ_{Boi} are assumed as the fractions of time for using auxiliary engines and boilers from the total navigation time. To estimate fuel consumption, we follow an approach similar to the IMO (2020), which incorporates ship's engine load, propulsive power demanded at different speeds, weather and fouling correction factors, auxiliary engines, and boilers, among others. Thus, the Admiralty formula with Equation (9) estimates the ship's main engine propulsive power demanded at a given speed. Since the specific fuel oil consumption of the main engine is varied as a function of its engine load parabolically (IMO 2020), SFC_{i,l_n}^{Main} is calculated with Equation (10), which is corrected with engine load (EL_{i,l_n}), given by $S_{t,l_n,i}^{Op}/S_i^d$ following Cariou et al. (2019).

$$Fuel_i = \sum_{n=1}^N (\delta_a^{HFO} \times (F_{l_n,i} \times FP_{MGO}) + (1 - \delta_a^{HFO}) (F_{l_n,i} \times FP_{HFO})) \quad \forall l_n \in a \quad (7)$$

$$F_{l_n,i} = \left((SFC_{i,l_n}^{Main} \times P_{i,l_n}^{Main}) + (\gamma_{Auc} \times SFC_i^d \times P_i^{AuxEng}) + (\gamma_{Boi} \times SFC_i^d \times P_i^{Boi}) \right) \times (D_i^{l_n} / S_{t,l_n,i}^{Op}) \quad (8)$$

$$P_{i,l_n}^{Main} = \frac{\delta_w \times P_{ref,i}^{Main} \times \left(\frac{S_{t,l_n,i}^{Op}}{S_i^d} \right)^n \times \left(\frac{drf_{i,l_n}}{drf_{ref,i}} \right)^m}{\eta_w \times \eta_f} \quad (9)$$

$$SFC_{i,l_n}^{Main} = SFC_{i,d}^{Main} \times (0.4551 \times EL_{i,l_n}^2 - 0.71 \times EL_{i,l_n} + 1.28) \quad (10)$$

$$Em_i = e_{Tax} \times \sum_{e=1}^4 \sum_{n=1}^N (\delta_a^{HFO} \times (F_{l_n,i} \times EF_{MGO,e} \times GWP_e) + (1 - \delta_a^{HFO}) (F_{l_n,i} \times EF_{HFO,e} \times GWP_e)) \quad \forall l_n \in a \quad (11)$$

$$IB_i = b_i \times B_n \times GT_i \quad (12)$$

Since we consider the impacts of emission tax as well, the total emission tax is given as the fourth component of Equation (4). Thus, after calculating the consumption of each fuel type, the total emission level is estimated incorporating different emission types (CO₂, CH₄, N₂O, and BC) and their emission factors with both HFO and MGO, which are converted into CO₂e using their global warming potential. Then, the total emission tax is estimated by Equation (11) considering the unit emission tax. As the last component of the cost function, ice-breaker cost is considered which is applicable in scenarios with medium and heavy-ice conditions. Thus, based on the collected ice-thickness data, if the ice-thickness level is in between I_i^2 and I_i^4 , the vessel is assumed to have ice-breaker assistance and the ice-breaker cost is estimated by Equation (12) considering the number of NSR's zones that require ice-breaker assistance, ice-breaker cost per NSR's zone per unit GT, and the GT of the vessel.

Deciding HFO-banned Areas

After deciding methods to estimate cost and emissions, an integer-programming optimization model is formulated to decide the optimum locations of HFO-banned areas to minimize total cost and emissions (CO₂e) as separate scenarios given with Equations (13) and (14). Equation (15) gives a binary constraint for selecting HFO-banned areas which is the decision variable for the optimization problem such that δ_a^{HFO} equals to 1 if area a is an HFO-banned area and 0 otherwise. Besides, Equation (16) gives a constraint on maximum allowable HFO-banned areas to test the model dynamics. Lastly, we consider a constraint on total SO_x emission as a fraction of total fuel consumption (Equation 17) where τ indicates the maximum allowable SO_x fraction. The developed model is solved with the Frontline Solver 2020 version with its Standard LP/Quadratic solver engine.

$$\min_{\delta_a^{HFO}} Cost_i = K_i + Oper_i + Fuel_i + Em_i + IB_i \quad (13)$$

$$\min_{\delta_a^{HFO}} Emission_i = \sum_{e=1}^4 \sum_{n=1}^N (\delta_a^{HFO} \times (F_{l_n,i} \times EF_{MGO,e} \times GWP_e) + (1 - \delta_a^{HFO}) (F_{l_n,i} \times EF_{HFO,e} \times GWP_e)) \quad \forall l_n \in a \quad (14)$$

$$\delta_a^{HFO} = \{0,1\} \quad (15)$$

$$\sum_{a=1}^M \delta_a^{HFO} \leq A_{max} \quad (16)$$

$$\sum_{n=1}^N (\delta_a^{HFO} \times (F_{l_n,i} \times EF_{MGO,SOx}) + (1 - \delta_a^{HFO}) (F_{l_n,i} \times EF_{HFO,SOx})) \leq \tau \times (\sum_{n=1}^N ((\delta_a^{HFO} \times F_{l_n,i}) + (1 - \delta_a^{HFO}) \times F_{l_n,i})) \quad \forall l_n \in a \quad (17)$$

RESULTS AND DISCUSSION

The proposed model from Equation (1) to (17) is tested with a selected voyage from Asia (Busan) and Europe (Bremerhaven) and the main input parameters are summarized in Table 1. Apart from them, based on the navigation path of the selected voyage, the numbers of legs (N) and potential HFO-banned areas that the vessel passing through (M) are found as 145 and 11 (A,B,C,E,G,H,J,M,P,O,Q), respectively. The average speed and navigation distance within each leg are calculated but not summarized here to maintain the brevity of this paper.

Table 1. Input parameters for the model

Type	Input Values
Vessel-specific Parameters	$GT:34882$; $Price_i^{NB} :5.5\text{MilUSD}$; $LT_i :10\text{years}$; $SFC_i^d:170 \text{ g/kWh}$; $S_i^d :19\text{knots}$; $S_i^{Min}:3\text{knots}$; $P_{ref}:31808\text{kW}$; $drf_{ref}:11\text{m}$; $P_i^{AuxEng}:1400\text{KW}$; $P_i^{Boi}:430\text{KW}$; $I_i^1:0.1\text{m}$; $I_i^2:0.3\text{m}$; $I_i^3:0.6$; $I_i^4:0.9\text{m}$ (AIS data and Cariou et al., 2019)
Model-specific Parameters	$\sigma:1.1$ (Otsuka et al., 2013); $\rho:1.25$ (Zhang et al., 2016); From IMO (2020) [$\eta_f:0.917$, $n:3$, $m:0.66$, $\gamma_{Auc}:0.5$, $\gamma_{Boi}:0.3$, $\eta_w:0.867$, $\delta_w:1$, $m:0.66$]; $A_{max}:10$ (base case); $\tau:0.04$ (base case)
Market-specific Parameters	$FP_{HFO} :600 \text{ USD/Ton}$; $FP_{MGO} :970 \text{ USD/Ton}$ (Cariou et al., 2018); $e_{Tax} :50 \text{ (USD/CO}_2\text{eTon)}$; Exchange rate (RUB/USD):75 (https://www.cbr.ru); Emission factors (g/gfuel) from IMO (2020) [$EF_{HFO,CO_2}:3.114$; $EF_{MGO,CO_2}:3.206$; $EF_{HFO,CH_4} :0.00006$; $EF_{MGO,CH_4} :0.00006$; $EF_{HFO,N_2O} :0.00016$; $E_{MGO,N_2O} :0.00015$; $EF_{HFO,BC} :0.00017$; $EF_{MGO,BC} :0.000004$; $EF_{HFO,SOx} :0.05083156$; $EF_{MGO,SOx} :0.001368542$]; GWP from IMO (2020) [$GWP_{CO_2}:1$, $GWP_{CH_4}:28$, $GWP_{N_2O}:265$, $GWP_{BC} :900$]

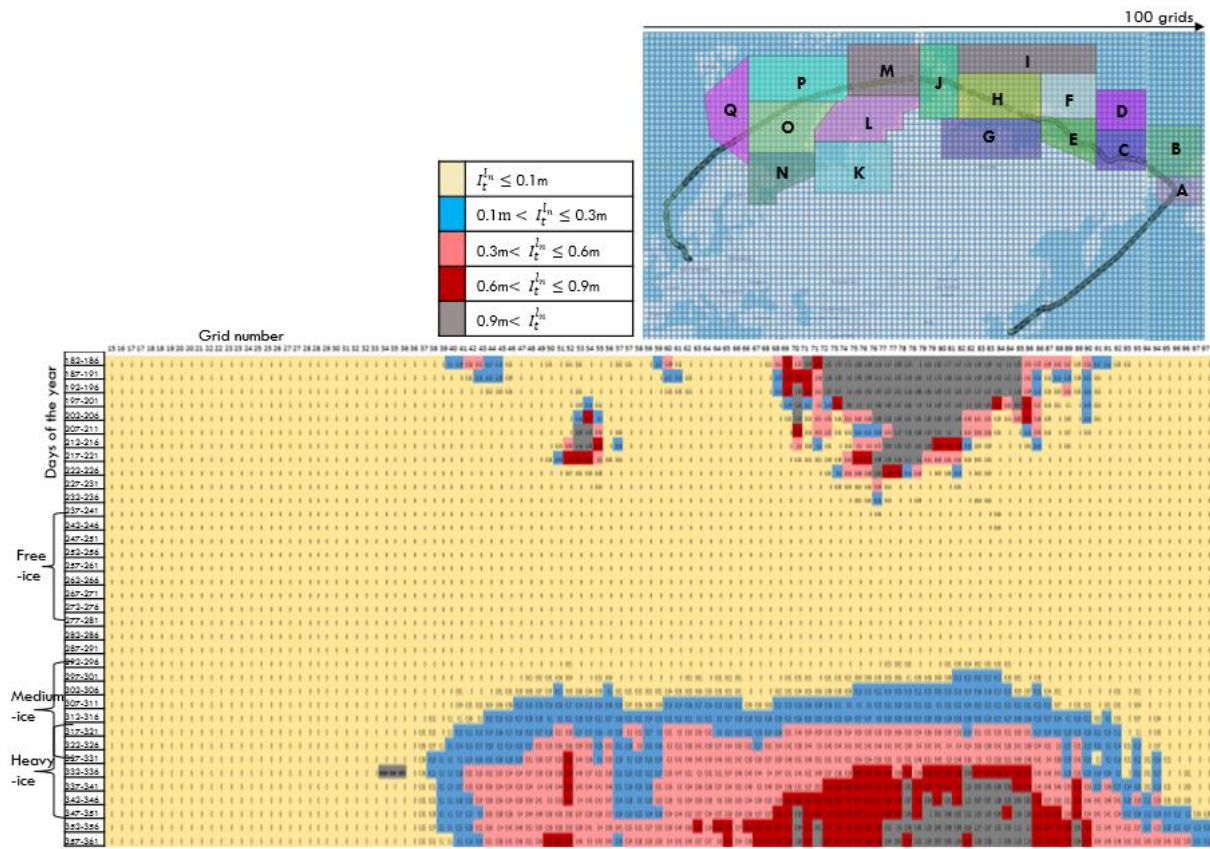


Figure 1. Ice-thickness data and potential HFO-banned areas along the navigation path

Figure 1 illustrates the spatial variation of ice-thickness level along the navigation path with potential HFO-banned areas decided for the analysis. Based on the ice-thickness level, we assumed three scenarios; free-ice scenario (voyage starting on day 240) based on actual navigation data from AIS, and medium-ice (voyage starting on day 297) and heavy-ice (voyage starting on day 317) scenarios with speeds estimated based on ice-thickness. However, these free-ice, medium-ice, and heavy-ice scenarios are subjective to the respective navigation path and different from the Russian classification on ice conditions. The total cost and emission of the voyage are estimated first without considering emission tax and HFO-banned areas and then with considering emission tax and HFO-banned areas. Table 2 summarizes the results without emission tax and HFO-banned areas and results with both minimizing cost and

minimizing emission when enforcing emission tax and HFO-banned areas. Accordingly, a significant reduction of SOx emission could be observed with both objectives along with a considerable reduction in CO2e levels. However, the total cost is increased significantly due to the emission tax and fuel switching inside HFO-banned areas although the rates of increase are almost similar among the three ice conditions. When comparing scenarios of ice-condition, a significant increase in cost with medium- and heavy-ice conditions reflects the cost of ice-breakers and changes in fuel cost and emission tax due to the variation of speed. Interestingly, the lowest emission level could be observed from the medium-ice scenario possibly due to the reduction of speeds with the presence of more ice than free-ice scenario and lesser ice than heavy-ice scenario which enables the vessel to have a longer independent navigation time even with slower speeds than the speed with ice-breaker assistance.

Table 2. Benefits of HFO-banned areas and emission tax

		Without HFO-banned areas and emission tax	When minimizing cost	When minimizing emission
Free-ice	Total cost (USD)	1457930.16	1784041.94	1862021.10
	CO2e (Tons)	4390.26	4372.82	4360.06
	SOx (Tons)	67.40	53.03	42.52
	Selected HFO-banned areas		A, B, C, H, J, Q	A, B, C, E, H, J, M, P, O, Q
Medium-ice	Total cost (USD)	1604280.18	1925518.27	1997694.70
	CO2e (Tons)	4324.00	4306.82	4295.01
	SOx (Tons)	66.38	52.23	42.50
	Selected HFO-banned areas		A, C, H, M, P	A, B, C, E, H, J, M, P, O, Q
Heavy-ice	Total cost (USD)	1658682.05	1985025.88	2063064.50
	CO2e (Tons)	4393.23	4375.77	4363.01
	SOx (Tons)	67.44	53.07	42.55
	Selected HFO-banned areas		B, C, G, H, J, P, O	A, B, C, E, H, J, M, P, O, Q

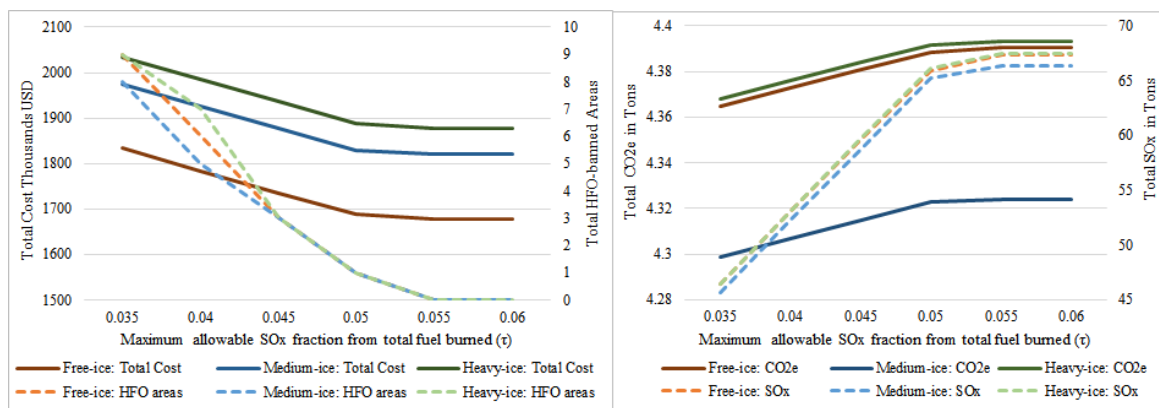


Figure 2. The sensitivity of maximum SOx fraction (τ) when minimizing total cost

Figure 2 summarizes results when minimizing the total cost with different values for maximum SOx fraction (τ). Accordingly, different numbers of HFO-banned areas are selected at three ice-conditions at small τ values (i.e. Six, five, and seven HFO-banned areas are selected at free, medium, and heavy ice-conditions, respectively when τ equals to 0.04). Further, total cost and CO2e among three scenarios follow similar variations when increasing the values of τ , highlighting the ineffectiveness of having a high value of τ for emission reduction despite the enforced emission tax. However, when minimizing total CO2e, all HFO-banned areas are

selected, thus the results with different number of maximum HFO-banned areas (A_{max}) are summarized in Figure 3 with the order of selecting HFO-banned areas. Accordingly, a trade-off relationship could be observed with cost and environmental objectives with all three ice-condition scenarios. Further, area H and G receive the highest and least priority, respectively for being selected as HFO-banned areas possibly due to the highest navigation length and considerable high average speed within area H and vice versa. Moreover, the locations of selected HFO-banned areas are varied when minimizing total CO₂e than minimizing the total cost, which can be considered in deciding mandatory vs voluntary fuel-switching policy.

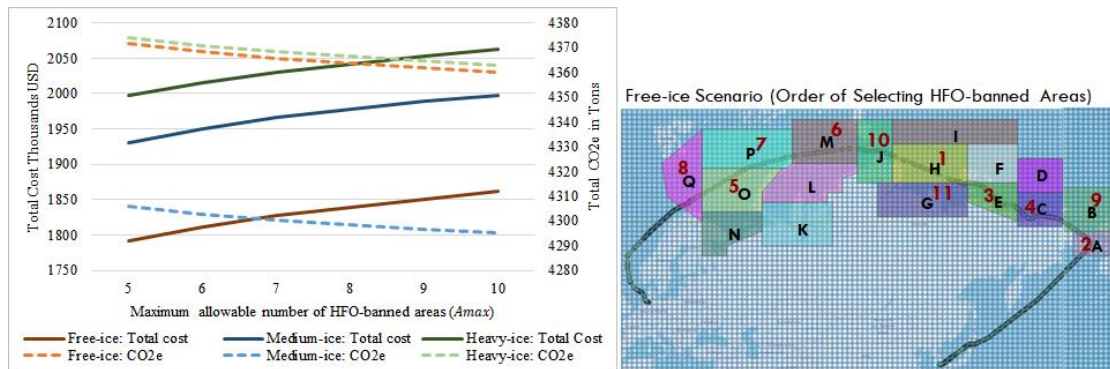


Figure 3. The sensitivity of maximum possible HFO-banned areas when minimizing CO₂e and order of selecting HFO-banned areas

Lastly, Figure 4 illustrates the spatial variation of selected HFO-banned areas under three ice-condition scenarios when minimizing total cost. Although areas H and C are selected with all three scenarios, the selection of other areas depends on the relevant ice-condition. For example, area J becomes an HFO-banned area under free-ice and heavy-ice conditions but not under the medium-ice condition because it has relatively higher speed due to the absence of ice under the free-ice condition and due to the ice-breaker assistance under heavy-ice condition, thus generates higher emissions than the emissions generated under medium-ice condition. Therefore, the voyage-based HFO-banned areas can be effectively decided based on the ice-condition at the time of navigation and the vessel-specific characteristics such as ice-strength level, engine power, among others.

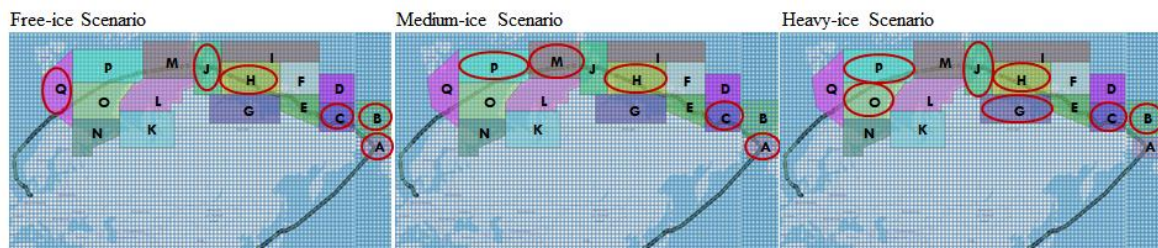


Figure 4. Spatial variation of selected HFO-banned areas when minimizing total cost

CONCLUSIONS

This study analyzes the effectiveness of enforcing HFO-banned areas and emission tax for enhancing the environmental sustainability of Arctic shipping and the optimum locations of HFO-banned areas are analyzed with both environmental and economic objectives. Results highlight a spatial variation of HFO-banned areas among free-ice, medium-ice, and heavy-ice scenarios with significant differences in cost and emission levels, and the medium-ice scenario

generates the least emission level. Although emission levels could be reduced by enforcing HFO-banned areas and emission tax, the total cost of the voyage increases significantly due to the fuel switching from HFO to MGO and emission tax. The average speed and voyage length inside an area have a significant influence on selecting it as an HFO-banned area. Further, an appropriate value on restricting SOx emission greatly influences the overall emission reduction from the voyage. Considering the significantly different results observed from environmental and economic objectives, the proposed voyage-based HFO-banned areas can be incorporated in formulating policy to advise vessels on voluntary or mandatory fuel-switching, respectively. Since emission tax also contributes to the high cost of the voyage, more sophisticated market-based measures such as emission trading system can be incorporated which generate better incentives for the voluntary fuel-switching by vessel operators. In future studies, the spatiotemporal variation of ice-concentration can be considered because we assumed 100% ice-concentration, which is a limitation of this study and HFO-banned areas can be decided considering all transit vessels simultaneously. The derived results can be compared with established navigation rules, databases, and maps from Russia on Arctic sea navigation.

REFERENCES

- Cariou, P., Cheaitou, A., Faury, O., & Hamdan, S., 2019. The feasibility of Arctic container shipping: the economic and environmental impacts of ice thickness. *Maritime Economics & Logistics*.
- Ding, W., Wang, Y., Dai, L., & Hu, H., 2020. Does a carbon tax affect the feasibility of Arctic shipping?. *Transportation Research Part D: Transport and Environment*. 80, 102257.
- IMO., 2020. Reduction of GHG emissions from ships: fourth IMO GHG study
- Lindstad, H., Bright, R.M., & Strømman, A.H., 2016. Economic savings linked to future Arctic shipping trade are at odds with climate change mitigation. *Transport Policy*, 45, pp.24-30.
- Otsuka, N., Izumiyama, K., & Furuichi, M., 2013. Study on Feasibility of the Northern Sea Route from Recent Voyages. *22nd International Conference on Port and Ocean Engineering under Arctic Conditions*. June 9-13, Espoo, Finland.
- The Japan Association of Marine Safety., 2015. Northern Sea Route Handbook.
- Faury, O., & P. Cariou., 2016. The Northern Sea Route competitiveness for oil tankers. *Transportation Research Part A: Policy and Practice*, 94, pp.461-469.
- Somanathan, S., Flynn, P., & J. Szymanski., 2009. The Northwest Passage: A simulation. *Transportation Research Part A: Policy and Practice*, 43, pp.127-135.
- Theocharis, D., Rodrigues, V.S., Stephen, P., & Haider, J., 2019. Feasibility of the Northern Sea Route: The role of distance, fuel prices, ice breaking fees and ship size for the product tanker market. *Transportation Research Part E: Logistics and Transportation Review*, 129, pp.111-135.
- Xu, H., Yang, D., & Weng, J., 2018. Economic feasibility of an NSR/SCR-combined container service on the Asia-Europe lane: a new approach dynamically considering sea ice extent. *Maritime Policy and Management*, 45(4), pp.514-529.
- Yumashev, D., Hussen, K.V., & 2 others., 2017. Towards a balanced view of Arctic shipping: estimating economic impacts of emissions from increased traffic on the Northern Sea Route. *Climatic Change*, 143, pp.143-155.

Zhang, Y., Meng, Q., & Ng, S.H., 2016. Shipping efficiency comparison between Northern Sea Route and the conventional Asia-Europe shipping route via Suez Canal. *Journal of Transport Geography*, 57, pp.241–249.

Zhang, Z., Huisingh, D., & Song, M., 2018. Exploitation of trans-Arctic maritime transportation. *Journal of Cleaner Production*, 212, pp.960-973.